Volume 1 | Number 1 | Jan 2013 | Pages 1–100

ChemComm

Chemical Communications
www.rsc.org/chemcomm

ROYAL SOCIETY OF CHEMISTRY

This is an *Accepted Manuscript*, which has been through the Royal Society of Chemistry peer review process and has been accepted for publication.

Accepted Manuscripts are published online shortly after acceptance, before technical editing, formatting and proof reading. Using this free service, authors can make their results available to the community, in citable form, before we publish the edited article. We will replace this *Accepted Manuscript* with the edited and formatted *Advance Article* as soon as it is available.

You can find more information about *Accepted Manuscripts* in the **Information for Authors**.

Please note that technical editing may introduce minor changes to the text and/or graphics, which may alter content. The journal's standard **Terms & Conditions** and the **Ethical guidelines** still apply. In no event shall the Royal Society of Chemistry be held responsible for any errors or omissions in this *Accepted Manuscript* or any consequences arising from the use of any information it contains.

Journal Name

COMMUNICATION

Facile Assembly of Light-Driven Molecular Motors onto a Solid Surface†

Jiawen Chen,‡ Kuang-Yen Chen,‡ Gregory T. Carroll and Ben L. Feringa*

In order to improve the rotary motion of surface assembled light-driven molecular motors, tetra-acid-functionalized motors were bound to an amine-coated quartz surface without prior activation of the acid groups. In contrast to earlier bipodal motors, the tetravalent motor showed no significant reduction in the rotation speed when attached to a surface.

A major challenge in nanotechnology is to build stimuli-responsive molecules to perform useful work.[1] Among the various organic molecules that have been proposed as components of future molecular devices and machines,[1] molecular motors based on overcrowded alkenes (motors) are highly promising systems.[2] These motors are able to convert light energy into repetitive unidirectional rotation, which occurs through a series of four steps involving photo-induced geometric isomerization and irreversible thermal isomerization reactions. It has been shown that molecular motors can be used to perform various tasks, such as propelling single molecules with control of directionality,[3a] controlling the chiral space in which a catalytic reaction takes place,[3b] inducing morphological changes in thin films,[3c] rotating micro-objects,[3d] and switching surface wettability in a reversible manner.[3e]

Brownian motion provides a considerable challenge to overcome in exploring possible applications that exploit the rotary cycle to power molecular devices. Both covalent[4] and non-covalent[5] approaches have been followed to confine stimuli-responsive molecules *i.e.* molecular machines, switches and rotors to surfaces. Multivalent surface attachment is essential in preventing uncontrolled Brownian motion around a single connection point. By confining rotary molecular motors on a surface, the relative rotation of one part of the molecule with respect to the other can be converted to absolute rotation of the rotor relative to the surface.[6a] We have previously designed a series of motors that can be attached to gold and quartz surfaces that bear alkyne, azide and amine functionalities *via* covalent binding. When these molecules are assembled at a surface,[3e,6] two types of orientations can be distinguished: azimuthal[6a,b] and altitudinal[3e,6c] (Figure 1a and 1b). Molecular motors with rotors in either orientation were shown to undergo rotary motion upon irradiation, however, the isomerization processes of previously designed bipodal motors were obstructed,

which was attributed to intermolecular interactions when they were confined to a crowded monolayer in comparison to their solution analogues (Figure 1b).[6c] Currently, among the key challenges in developing surface-bound devices based on molecular motors is the development of efficient strategies for surface functionalization and demonstrating unobstructed rotary motion in surface-bound systems. Recently we followed a covalent approach by designing a tripodal molecular motor system in order to create free volume between the surface-bound motors, allowing enhanced switching behaviour.[3e] Assembly of molecular devices at an interface, taking advantage of non-covalent interactions, holds promise as was elegantly shown by Leigh *et. al.* for a rotaxane-based system capable of transporting droplets.[5c] We were encouraged by a recent report by Hofkens, Müllen *et al.* on a tripodal molecular rotor which can be assembled directly onto a negatively-charged glass surface *via* a positively-charged tripodal unit by non-covalent interactions.[5d] The attachment of the rotor to the interface appears to be robust, and defocused wide-field fluoresence microscopy showed that the rotor can rotate freely on the surface without significant loss of binding.
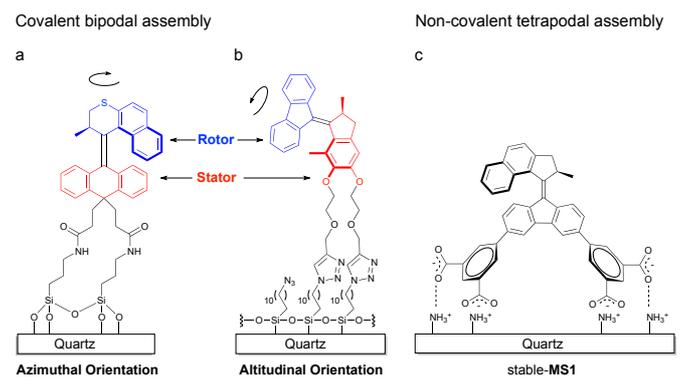

Figure 1 (a) Azimuthal and (b) altitudinal rotary motors on surfaces. (c) Assembly of tetrapodal motor **1** on amine-functionalized quartz.

Here we report novel molecular motors containing a multivalent stator functionalized with acid groups for electrostatic attachment to amine-coated quartz (Figure 1c; for synthesis see ESI†).[5a,6b] The carboxylic acids do not require further activation

prior to surface preparation, making this system advantageous over a previously reported system involving amide formation of carboxylic acid functionalized motors with amine-coated quartz *via* an unstable acid chloride intermediate (Figure 1a).[6b] Reduction in rotary speed can be overcome by designing motors **1** with tetravalent stators to increase the free volume between the surface-bound motors and therefore minimize intermolecular interactions while simultaneously the orientation is more firmly controlled by the rigid tetrapodal structure.[3e] Molecular models show that meta-substitution of each biaryl unit in the stator part of **1** with two carboxylates favours an azimuthal orientation of the rotor relative to the surface (Figure 1c). A related bivalent motor **2** was also prepared, in order to compare the effect of the valency of surface attachment on the rotary speed of the surface-bound motors. The photochemically and thermally driven isomerizations (Scheme 1a) of these tetra- and bi-valent motors **1** and **2** were compared both in solution and when attached to quartz surfaces.

1: R₁ = R₂ = CO₂H   2: R₁ = H, R₂ = CO₂H
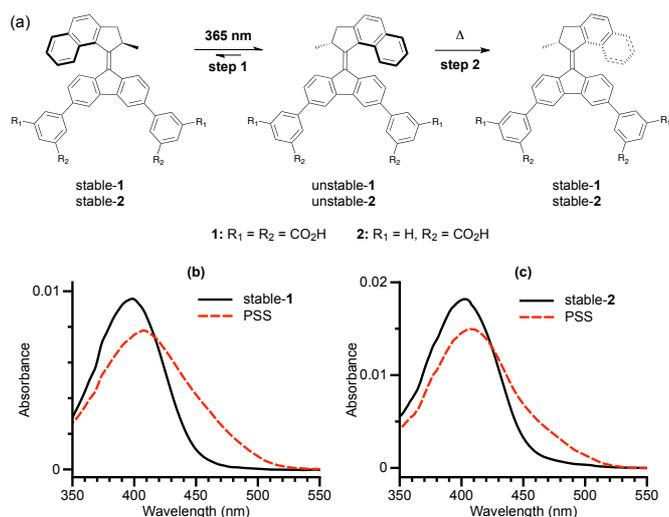
Scheme 1 (a) Photochemical and thermal isomerization steps of motors **1** and **2**; UV/vis absorption spectra (MeOH, 278 K) of stable-**1** (b) and stable-**2** (c) before irradiation (solid lines) and at the photostationary state (PSS) (dashed lines).

The photochemical and thermal properties of molecular motors **1** and **2** were analysed by UV/vis absorption spectroscopy. The UV/vis spectra of stable-**1** (2.02×10^{-6} M) and stable-**2** (1.92×10^{-6} M) in MeOH at 278 K both show absorption bands centred at 399 and 402 nm, respectively (Scheme 1b and 1c, solid lines).

Irradiation with UV light ($\lambda_{max} = 365$ nm) led to a red-shift of the bands at 399 and 402 nm, indicating photochemically induced formation of the unstable isomer (Scheme 1a, step 1). This red shift is consistent with increased strain at the central double bond, and hence the generation of an isomer with a higher energy ground state.[2] During irradiation, isosbestic points were maintained in each case. Each sample was irradiated until no further change was observed, *i.e.* the photostationary state (PSS) was reached (Scheme 1b and 1c, dashed lines). Allowing the PSS mixture of stable-**1**/unstable-**1** or stable-**2**/unstable-**2** to warm to rt resulted in a blue-shift of the bands to their original positions at 399 and 402 nm, which is consistent with thermal isomerization back to the corresponding stable isomers (Scheme 1a, step 2).

Kinetic analyses were performed on the thermal isomerization steps of both motors at several temperatures (Scheme 1a, step 2; Figure S2, ESI†). For unstable-**1** → stable-**1**, the Gibbs free energy of activation ($\Delta^{\ddagger}G^o$) was calculated to be

84.5 kJ/mol (half-life $t_{1/2} = 130$ s at 293 K) and for unstable-**2** → stable-**2**, $\Delta^{\ddagger}G^o$ was calculated to be 86.0 kJ/mol ($t_{1/2} = 227$ s at 293 K). These values are similar to those obtained from structurally related motors.[3a,3e,6c]

By studying the photochemical and thermal behaviour of **1** and **2** using UV/vis absorption spectroscopy, and by analogy with motor systems reported previously,[3a,3e,6c] it was shown that **1** and **2** function as light-driven rotary motors in solution. The introduction of the carboxylic acid groups on the motor moiety does not have a significant influence on the photochemical and thermal behaviour of the molecular motors.

In order to compare the photochemical and thermal behaviour of the motors in solution to those on the surfaces, surface-attached motor assemblies **MS1** and **MS2** were prepared (Figure 1c; **MS** = **M**otor on **S**urface). Following literature procedures,[3e] amine-coated quartz were prepared by immersing piranha-cleaned quartz slides in a 1 mM solution of 3-aminopropyl(diethoxy)methylsilane in toluene at rt for 12 h. The substrates were then rinsed extensively with toluene and MeOH and dried under a stream of argon. Motors **1** and **2** were grafted to amine-coated quartz by immersing the slides in a solution of CH_2Cl_2 (10^{-4} M) containing stable-**1** or stable-**2** at rt for 6-24 h, followed by extensive rinsing with CH_2Cl_2 and drying under a stream of argon.

The presence of the motor on the surface was confirmed by UV/vis absorption spectroscopy and water contact angle measurements. The UV/vis absorption spectra of stable-**MS1** or stable-**MS2** showed the characteristic absorption bands of the motors (Figure 2, solid lines). The major absorption band and the absorption profile are similar to that observed in MeOH solution (Scheme 1b and 1c, solid lines), showing that the motors were attached to the amine-coated quartz successfully. No changes in UV/vis absorption were observed after 10 h immersion time (Figure S4, ESI†) indicating that complete coverage of the surfaces is reached.
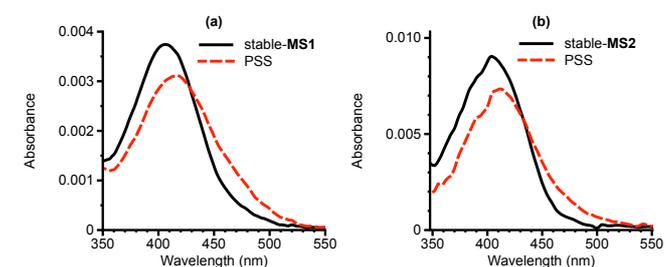

Figure 2 UV/vis absorption spectra (278 K) of stable-**MS1** (a) and stable-**MS2** (b) before irradiation (solid line) and at the photostationary state (dashed line).

Water contact angles (WCA) of the amine and motor-coated surfaces were determined by contact-angle goniometry studies using the Sessile drop method.[7] Coating an amine-functionalized surface with molecular motor **1** or **2** resulted in an increase in WCA from $40 \pm 1°$ for the amine-modified surface to $63 \pm 1°$ and $73 \pm 1°$ for **MS1** and **MS2**, respectively (Figure 3). The lower WCA of **MS1** compared to **MS2** is likely due to the presence of two additional carboxylic acids per motor and the additional free volume between the surface-bound motors, which might allow the water to more easily access free amine groups.

Figure 3 Water droplets on amine-coated quartz (left), **MS1** (middle), and **MS2** (right). The measured water contact angles are 40°, 63° and 73°, respectively.

Irradiation of stable-**MS1** and stable-**MS2** with UV light for 15 min (λ_{max} = 365 nm, 278 K, N_2 atmosphere), led to a red-shift in the long-wavelength bands in the UV/vis absorption spectra (Figure 2, dashed lines), indicating the formation of the unstable-isomers of the surface-bound motors (Scheme 1a, step 1; stable-**MS1** → unstable-**MS1** and stable-**MS2** → unstable-**MS2**). Allowing the substrate to warm to rt restored the original spectra, indicating thermal isomerization back to stable-**MS1** and stable-**MS2** (Scheme 1a, step 1). These observations are consistent with the thermal behaviour of unstable-**1** and unstable-**2** in MeOH.

Whether or not the surface immobilization compromises the rotary speed of the motors was determined by the thermal isomerization step (Scheme 1a, step 2) by monitoring the decay of the absorbance at 475 nm as a function of time (Figure S3, ESI†). The decrease in the absorbance for unstable-**MS1** → stable-**MS1** was fitted with a monoexponential decay, as for its solution analogue (Figures S2a, ESI†), and a half-life ($t_{1/2}$ = 161 s at rt) was determined This value is similar to the half-life observed in MeOH solution for unstable-**1** → stable-**1** ($t_{1/2}$ = 130 s at rt), indicating that the rotary motion of the tetravalent motor **1** shows minimal, if any, inhibition from neighbouring surface-bound motors.

However, in contrast to solution phase experiments, the thermal isomerization data for unstable-**MS2** → stable-**MS2** suggests more complicated dynamics for the bipodal motor **2** assembled to the surface. The time dependent change in the absorbance at 475 nm was found to fit a biexponential decay and two-half lives were found that differ by an order of magnitude at 293 K, suggesting that at least two processes occurred during thermal isomerization. The first half-life had a value of 544 s, which is significantly longer than the half-life observed as a result of unstable-**2** → stable-**2** isomerization in solution ($t_{1/2}$ = 227 s at 293 K). The second half-life has a value of 3855 s, which indicates the thermal isomerization of the surface-bound motor **MS2** is slowed down considerably compared to the solution analogue.

The UV/vis absorption of **MS1** is lower in intensity than for **MS2** (Figure 2). We attribute the lower UV/vis signal to a lower surface coverage, although surface orientation can also affect the UV/vis absorbance. The lower surface coverage for **MS1** can be attributed to the specific architecture featuring the twisting of the meta-dicarboxylate functionalized phenyl moieties approximately 90 ° relative to the fluorene stator, allowing tetrapodal binding to the surface, while creating more free volume between the rotors and forcing the motors to stand upright. In the case of bipodal **MS2**, the surface-binding benzoic acid units occupy less space but besides molecular size and packing density, also flexibility is expected to play an important role as **MS2** can readily adopt several conformations at the surface in contrast to more rigid **MS1**. The detection of different isomerization processes for **MS2** might be attributed to interference of motors in the more densely packed monolayer, as seen before with bipodal altitudinal motors[6c] or different conformations at the surface. The more complicated non-monoexponential kinetics may reflect a non-uniform distribution and inhomogeneity (*i.e.* various tilt angles, inter-molecular interactions, distinct conformations). Non-monoexponential kinetics were previously observed for bipodal motors[6c] and side chain, azobenzene-functionalized polymer films.[8] The rate of thermal *cis* → *trans* isomerization in these azobenzene films was found to deviate from a simple monoexponential decay due to neighbouring effects on the motion of the azobenzene groups. Our results, based on the new design of surfaced assembled tetrapodal motor **MS1,** demonstrate that well-defined assemblies can be readily obtained

and unobstructed rotary motion, comparable to the related system in solution, can be achieved.

In conclusion, we described a novel tetrapodal motor designed with improved control over the surface assembly of light-driven molecular motors. The four carboxylic acid groups at the stator allow for the motors to be attached to surfaces bearing amines without the need to activate the carboxylic acid (Figure 1a). The motors preserve their rotary function and thermal isomerization of **MS1** containing a tetravalent stator was not inhibited significantly by surface immobilization. This study demonstrates how differences in molecular anchoring can considerably impact dynamic processes of surface assembled nanoscale motors. The new design features will be key in our ongoing studies towards developing more advanced, dynamic surface-anchored systems.

Notes and references

Stratingh Institute for Chemistry, University of Groningen, Nijenborgh 4, 9747AG Groningen, The Netherlands. Tel: +31 50 3634278; Fax: +31 50 3634296; Email: b.l.feringa@rug.nl

‡ Co-first authors.

1 (a) K. Kinbara, T. Aida, *Chem. Rev.* 2005, **105**, 1377-1400. (b) S. Saha and J. F. Stoddart, *Chem. Soc. Rev.*, 2007, **36**, 77–92. (c) W. R. Browne and B. L. Feringa, *Nat. Nanotechnol.*, 2006, **1**, 25–35. (d) E. R. Kay, D. A. Leigh, and F. Zerbetto, *Angew. Chem. Int. Ed.*, 2007, **46**, 72–191. (e) *Molecular Devices and Machines: Concepts and Perspectives for the Nanoworld*, ed. V. Balzani, A. Credi, and M. Venturi, Wiley-VCH, Weinheim, 2008. (f) A. Coskun, M. Banaszak, R. D. Astumian, J. F. Stoddart, and B. A. Grzybowski, *Chem. Soc. Rev.*, 2012, **41**, 19–30.

2 (a) N. Koumura, R. W. Zijlstra, R. A. van Delden, N. Harada, and B. L. Feringa, *Nature*, 1999, **401**, 152–155. (b) N. Koumura, E. M. Geertsema, M. B. van Gelder, A. Meetsma, and B. L. Feringa, *J. Am. Chem. Soc.*, 2002, **124**, 5037–5051.

3 (a) T. Kudernac, N. Ruangsupapichat, M. Parschau, B. Maciá, N. Katsonis, S. R. Harutyunyan, K.-H. Ernst, and B. L. Feringa, *Nature*, 2011, **479**, 208–211. (b) J. Wang and B. L. Feringa, *Science*, 2011, **331**, 1429–1432. (c) G. London, G. T. Carroll and B. L. Feringa, *Org. Biomol. Chem.*, 2013, **11**, 3477–3483. (d) R. Eelkema, M. M. Pollard, J. Vicario, N. Katsonis, B. S. Ramon, C. W. M. Bastiaansen, D. J. Broer, and B. L. Feringa, *Nature*, 2006, **440**, 163–163. (e) K.-Y. Chen, O. Ivashenko, G. T. Carroll, J. Robertus, J. C. M. Kistemaker, G. London, W. R. Browne, P. Rudolf, and B. L. Feringa, *J. Am. Chem. Soc.*, 2014, **136**, 3219–3224. (For a tripodal azobenzene, see 4f)

4 (a) J. Michl and E. C. H. Sykes, *ACS Nano*, 2009, **3**, 1042–1048. (b) U. G. E. Perera, F. Ample, H. Kersell, Y. Zhang, G. Vives, J. Echeverria, M. Grisolia, G. Rapenne, C. Joachim, and S.-W. Hla, *Nat. Nanotechnol.*, 2013, **8**, 46–51. (c) J. Puigmartí-Luis, W. J. Saletra, A. González, D. B. Amabilino, and L. Pérez-García, *Chem. Commun.*, 2013, **50**, 82-84. (d) V. Balzani, A. Credi, M. Venturi, *ChemPhysChem*, 2008, **9**, 202-220. (e)

ChemComm Accepted Manuscript

G. S. Kottas, L. I. Clarke, D. Horinek, J. Michl, *Chem. Rev.* 2005, **105**, 1281-1376. (f) T. Y. Huang, B. Brough, C.-M. Ho, Y. Liu, A. H. Flood, P. A. Bonvallet, H.-R. Tseng, J. F. Stoddart, M. Ballaer, S. Magonov, *Appl. Phys. Lett.* 2004, **85**, 5391-5393. (g) J. Vacek, J. Michl, *Adv. Funct. Mater.* 2007, **17**, 730-739. (f) S. Wagner, F. Leyssner, C. Kördel, S. Zarwell, R. Schmidt, M. Weinelt, K. Rück-Braun, M. Wolf, and P. Tegeder, *Phys. Chem. Chem. Phys.*, 2009, **11**, 6242–6248.

5 (a) *From Non-Covalent Assemblies to Molecular Machines*, ed. J.-P. Sauvage, and P. Gaspard, Wiley-VCH, Weinheim, 2010. (b) P. F. Driscoll, N. Purohit, N. Wanichacheva, C. R. Lambert, W. G. McGimpsey, *Langmuir* 2007, **23**, 3181-13187. (c) J. Berná, D. A. Leigh, M. Lubomska, S. M. Mendoza, E. M. Pérez, P. Rudolf, G. Teobaldi, and F. Zerbetto, *Nat. Mater.*, 2005, **4**, 704–710. (d) J. A. Hutchison, H. Uji-i, A. Deres, T. Vosch, S. Rocha, S. Müller, A. A. Bastian, J. Enderlein, H. Nourouzi, C. Li, A. Herrmann, K. Müllen, F. De Schryver, and J. Hofkens, *Nat. Nanotechnol.*, 2014, **9**, 131–136.

6 (a) R. A. van Delden, M. K. J. ter Wiel, M. M. Pollard, J. Vicario, N. Koumura, and B. L. Feringa, *Nature*, 2005, **437**, 1337–1340. (b) M. M. Pollard, M. Lubomska, P. Rudolf, and B. L. Feringa, *Angew. Chem.*, 2007, **119**, 1300–1302. (c) G. T. Carroll, G. London, T. F. Landaluce, P. Rudolf, and B. L. Feringa, *ACS Nano*, 2011, **5**, 622–630.

7 O. Ivashenko, H. Logtenberg, J. Areephong, A. C. Coleman, P. V. Wesenhagen, E. M. Geertsema, N. Heureux, B. L. Feringa, P. Rudolf, and W. R. Browne, *J. Phys. Chem. C*, 2011, **115**, 22965–22975.

8 (a) C. Barrett, A. Natansohn, and P. Rochon, *Macromolecules*, 1994, **27**, 4781–4786. (b) A. Priimagi, K. Lindfors, M. Kaivola, and P. Rochon, *ACS Appl. Mater. Interfaces*, 2009, **1**, 1183–1189.